

ORIGINAL ARTICLE

Synthesis and properties of novel network polymers containing castor oil and silsesquioxane moieties

Nozomu Uchida and Hiroaki Kouzai

Novel network polymer precursors were synthesized with castor oil or branched poly(L-lactic acid) and 3-(triethoxysilyl)propyl isocyanate. The network polymer precursors were cross-linked at 120 °C for 24 h to obtain network polymer films. The film formed from castor oil was easily broken when peeled off of a polytetrafluoroethylene petri dish, while the film formed from branched poly(L-lactic acid) was obtained as a self-supporting film. Thermal stabilities of the obtained films were measured by thermogravimetric analysis. The temperature at which 10% weight loss (T_{d10}) occurred was 298 °C for the film derived from castor oil, and the T_{d10} of the film made from branched poly(L-lactic acid) was 200 °C. The film obtained using branched poly(L-lactic acid) exhibited elastomeric properties owing to a relatively low glass transition temperature of 3 °C and the onset of a rubbery plateau region at approximately 20 °C, as measured by dynamic mechanical analysis. Furthermore, we also prepared a film using the precursor material together with tetraethyl orthosilicate. The obtained film exhibited a higher thermal stability ($T_{d10} = 223$ °C) than that of the film using branched poly(L-lactic acid). Finally, the cross-linked films were subjected to degradation by exposure to porcine pancreas lipase. The observation of weight loss after 30 days confirmed the degradability of the films.

Polymer Journal (2016) 48, 703–708; doi:10.1038/pj.2016.11; published online 17 February 2016

INTRODUCTION

Polymers derived from petroleum resources have been widely used in a broad range of applications in the form of elastomers, fibers, foams, coatings and biomedical materials owing to their high thermal stabilities, high durability and lightweight properties. In general, these polymers are not environmentally degradable because of their high chemical stability. As a result, polymer waste streams are currently subjected to thermal recycling by a combustion treatment process, which has led to increased carbon dioxide emissions and has become a point of contention for environmental issues, such as global warming. Consequently, biomass-derived polymers have gained the attention of many researchers in recent years as environmentally friendly materials.^{1–12} The use of biomass polymers is expected to make a significant contribution toward reduction of carbon dioxide emissions because biomass is a renewable resource. However, the majority of general biomass polymers are typically hard and brittle plastics, poly(L-lactic acid) (PLLA) being a well-known example. Accordingly, polymers that exhibit these properties are only useful for a narrow range of applications. In this study, we therefore focused on the use of castor oil to address the problem of low elasticity in biodegradable polymers. Castor oil is a polyol obtained from *Ricinus communis* seeds, and polymers derived from castor oil are highly flexible by virtue of the incorporation of long aliphatic chains.^{13–18} For this reason, castor oil is a suitable material for the modification of brittle polymers. Research on polymers derived from castor oil has generally focused on

utilizing its hydroxyl groups to synthesize polyurethanes. It is important to explore the use of castor oil for the synthesis of novel polymers beyond simply polyurethanes, however, to realize the potential of biomass polymers for various applications. Cross-linked polymers are tough and exhibit elastomeric properties. We have already reported a novel network polymer using branched PLLA derived from castor oil and 2-acryloyloxyethyl isocyanate.¹⁹ Although biomass polymers prepared using castor oil contribute toward reducing the environmental impact of polymers as described above, they tend to be poorly thermally stable, limiting their practical utility. To address this problem, we envisioned combining the biodegradability of biomass polymers with the desirable properties of silicon-based polymers to form high-performance silicon-based hybrid polymers. Polymers containing inorganic elements are known to exhibit desirable or useful properties.^{20–24} For example, polymers containing Si moieties generally have a high thermal stability as well as highly adhesive properties. Among such polymers, polysilsesquioxane has been studied by many groups.^{25–34} This is because these polymers can be synthesized by simple methods using silane coupling agents. Moreover, polysilsesquioxanes have already been commercialized for applications, such as low pollution paints and hard coatings.

Accordingly, we carried out the synthesis and characterization of a novel network polymer using castor oil and 3-(triethoxysilyl)propyl isocyanate with the goal of developing a high-performance biomass

polymer. Furthermore, the degradability of the synthesized polymers was confirmed by enzyme hydrolysis.

EXPERIMENTAL PROCEDURE

Materials

Castor oil (hydroxyl value = 161.2 mg KOH per gram) was a gift from Itoh Oil Chemicals (Japan). The number-average molecular weight of castor oil was 950 (determined by gel permeation chromatography). The structure of castor oil was confirmed by ^1H NMR spectroscopy. The chemical shifts are assigned as follows: ^1H NMR (δ , p.p.m. from tetramethylsilane (TMS) in CDCl_3): 0.9 (t, $-\text{CH}_2 \text{CH}_3$), 1.3 (m, $-\text{CH}_2 \text{CH}_2 \text{CH}_2-$), 1.4 (m, $-\text{CH}_2 \text{CH}_2 \text{CH}_2-$), 1.6 (m, $-\text{CH}_2 \text{CH}_2 \text{CH}_2-$), 2.0 (t, $-\text{CH}_2 \text{CH}=\text{CH}-$), 2.2 (t, $=\text{CH} \text{CH}_2 \text{CH}(\text{OH})-$), 2.3 (q, $-\text{C}(\text{O}) \text{CH}_2 \text{CH}_2-$), 3.6 (m, $-\text{CH}_2 \text{CH}(\text{OH}) \text{CH}_2-$), 4.1 (m, $-\text{CH}(\text{OH}) \text{CH}_2 \text{CH}_2$), 4.3 (m, $-\text{CH} \text{CH}_2 \text{O}-$), 5.2 (m, $-\text{CH}_2 \text{CH}(\text{O} \text{C} \text{O} \text{CH}_2-) \text{CH}_2-$), 5.4 (m, $-\text{CH}=\text{CH}-$), 5.6 (m, $-\text{CH}=\text{CH}-$). The *l*-lactide (>98.0%), 3-(triethoxysilyl)propyl isocyanate (>95.0%), dibutyltin dilaurate (>95.0%), tetraethyl orthosilicate (>96.0%) and porcine pancreas lipase were purchased from Tokyo Chemical Industry (Tokyo, Japan). Disodium hydrogen phosphate (>99.0%) and potassium dihydrogen phosphate (>99.0%) were purchased from Wako Pure Chemical Industries (Osaka, Japan). Tin 2-ethylhexanoate (>92.5%) was purchased from Sigma-Aldrich Japan (Tokyo, Japan). All the other reagents and solvents are commercially available and were used as received.

Synthesis of branched PLLA (COLA) (1)

COLA was synthesized according to ref. 19. All synthetic routes are shown in Figure 1. A typical process is described as follows: castor oil (1.9 g, 2.0 mmol) was reacted with *l*-lactide (5.8 g, 40.0 mmol) for 5 h at 140 °C in the presence of tin 2-ethylhexanoate as a catalyst under a nitrogen atmosphere. After completion of the reaction, the product was precipitated into hexane and dried under vacuum.

^1H NMR (δ , p.p.m. from TMS in CDCl_3): 0.9 (t, $-\text{CH}_2 \text{CH}_3$), 1.3 (m, $-\text{CH}_2 \text{CH}_2 \text{CH}_2-$), 1.4 (m, $-\text{CH}_2 \text{CH}_2 \text{CH}_2-$), 1.6 (m, $-\text{CH}_2 \text{CH}_2 \text{CH}_2-$, $-\text{CH}-\text{CH}_3$), 2.0 (t, $-\text{CH}_2 \text{CH}=\text{CH}-$), 2.3 (q, $-\text{C}(\text{O}) \text{CH}_2 \text{CH}_2-$), 4.1 (m, $-\text{CH}(\text{O} \text{C} \text{O}-) \text{CH}_2 \text{CH}_2-$), 4.3 (m, $-\text{CH} \text{CH}_2 \text{O}-$), 4.9 (m, $-\text{CH}_2 \text{CH}(\text{O} \text{C} \text{O}-) \text{CH}_2-$), 5.1–5.2 (m, $-\text{CH}_2 \text{CH}(\text{O} \text{C} \text{O} \text{CH}_2-) \text{CH}_2-$, $-\text{O} \text{C}(\text{O}) \text{CH}(\text{CH}_3) \text{C}(\text{O})-$), 5.4 (m, $-\text{CH}=\text{CH}-$), 5.6 (m, $-\text{CH}=\text{CH}-$).

Synthesis of castor oil-modified triethoxysilane (CO-TES) (2)

Under an argon atmosphere, 3-(triethoxysilyl)propyl isocyanate (0.74 g, 3.0 mmol) and castor oil (0.95 g, 1.0 mmol) were dissolved in chloroform (CHCl_3) (2.0 ml). The solution was stirred at room temperature for 0.5 h, and dibutyltin dilaurate, which was used as a catalyst, was added dropwise. The mixture was stirred for 24 h, at which point the solvent was evaporated, and the product was washed with hexane and dried under vacuum.

^1H NMR (δ , p.p.m. from TMS in CDCl_3): 0.6 (q, $-\text{CH}_2 \text{CH}_2 \text{Si}-$), 0.9 (t, $-\text{CH}_2 \text{CH}_3$), 1.3–1.6 (m, $-\text{CH}_2 \text{CH}_2 \text{CH}_2-$, $-\text{Si} \text{CH}_2 \text{CH}_3$), 2.0 (t, $-\text{CH}_2 \text{CH}=\text{CH}-$), 2.3 (q, $-\text{C}(\text{O}) \text{CH}_2 \text{CH}_2-$), 3.2 (t, $-\text{C}(\text{O}) \text{NH} \text{CH}_2-$), 3.8 (m, $-\text{Si} \text{O} \text{CH}_2 \text{CH}_3$), 4.1 (m, $-\text{CH}(\text{O} \text{C} \text{O}-) \text{CH}_2 \text{CH}_2-$), 4.3 (m, $-\text{CH} \text{CH}_2 \text{O}-$), 4.9 (m, $-\text{CH}_2 \text{CH}(\text{O} \text{C} \text{O}-) \text{CH}_2-$), 5.2 (m, $-\text{CH}_2 \text{CH}(\text{O} \text{C} \text{O} \text{CH}_2-) \text{CH}_2-$), 5.4 (m, $-\text{CH}=\text{CH}-$), 5.6 (m, $-\text{CH}=\text{CH}-$).

Synthesis of COLA-modified triethoxysilane (COLA-TES) (3)

3-(Triethoxysilyl)propyl isocyanate (0.14 g, 0.6 mmol) and COLA (1.14 g, 0.2 mmol) were dissolved in CHCl_3 (2.0 ml). The solution was stirred at room temperature for 0.5 h, and dibutyltin dilaurate, which was used as a catalyst, was added dropwise. The mixture was stirred for 24 h, at which point the solvent was evaporated, and the product was washed with hexane and dried under vacuum.

^1H NMR (δ , p.p.m. from TMS in CDCl_3): 0.6 (q, $-\text{CH}_2 \text{CH}_2 \text{Si}-$), 0.9 (t, $-\text{CH}_2 \text{CH}_3$), 1.2–1.5 (m, $-\text{CH}_2 \text{CH}_2 \text{CH}_2-$, $-\text{Si} \text{CH}_2 \text{CH}_3$), 1.6 (m, $-\text{CH}_2 \text{CH}_2 \text{CH}_2-$, $-\text{CH} \text{CH}_3$), 2.0 (t, $-\text{CH}_2 \text{CH}=\text{CH}-$), 2.3 (q, $-\text{C}(\text{O}) \text{CH}_2 \text{CH}_2-$), 3.2 (t, $-\text{C}(\text{O}) \text{NH} \text{CH}_2-$), 3.8 (m, $-\text{Si} \text{O} \text{CH}_2 \text{CH}_3$), 4.1 (m, $-\text{CH}(\text{OH}) \text{CH}_2 \text{CH}_2-$), 4.2–4.4 (m, $-\text{CH} \text{CH}_2 \text{O}-$), 4.9 (m, $-\text{CH}_2 \text{CH}(\text{O} \text{C} \text{O}-) \text{CH}_2-$), 5.1–5.2 (m, $-\text{CH}_2 \text{CH}(\text{O} \text{C} \text{O} \text{CH}_2-) \text{CH}_2-$, $-\text{O} \text{C}(\text{O}) \text{CH}(\text{CH}_3) \text{C}(\text{O})-$), 5.3 (m, $-\text{CH}=\text{CH}-$), 5.5 (m, $-\text{CH}=\text{CH}-$).

Cross-linking reaction of CO-TES (Film 1)

CO-TES (0.95 g, 1.0 mmol) was dissolved in tetrahydrofuran (1.0 ml). Pure water and triethylamine as a catalyst were added dropwise into the solution. The mixture was then dried and cured at 40 °C for 3 h in a polytetrafluoroethylene (PTFE) petri dish. Further cross-linking was carried out at 120 °C for 24 h. The cross-linked film was dipped in organic solvent to wash and dried under vacuum.

Fourier transform infrared (FT-IR) spectroscopy (ATR, cm^{-1}): 3350 ($-\text{NH}-$), 2940 ($-\text{CH}_2-$), 1750 ($-\text{CO}-\text{O}-$).

Cross-linking reaction of COLA-TES (Film 2)

The cross-linking of COLA-TES was performed in the same way as Film 1. Briefly, COLA-TES (1.0 g, 0.2 mmol) was dissolved in tetrahydrofuran (1.0 ml). Pure water and triethylamine as a catalyst were added dropwise to the solution. The mixture was then dried and cured at 40 °C for 3 h in a PTFE petri dish. Further cross-linking was carried out at 120 °C for 24 h. The cross-linked film was dipped in organic solvent to wash and dried under vacuum. FT-IR (ATR): 3320 ($-\text{NH}-$), 2920 ($-\text{CH}_2-$), 1750 ($-\text{CO}-\text{O}-$) cm^{-1} .

Cross-linking reaction of COLA-TES and tetraethyl orthosilicate (Film 3)

We also carried out the cross-linking reaction using tetraethyl orthosilicate, which resulted in an increased number of inorganic moieties in the film

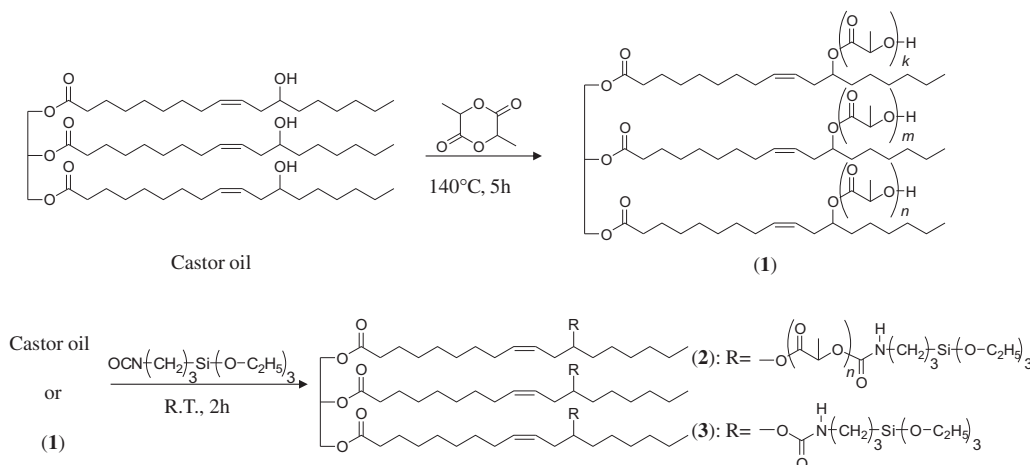


Figure 1 Synthesis of COLA (1), CO-TES (2) and COLA-TES (3).

compared with the above method. COLA-TES (1.0 g, 0.2 mmol) and tetraethyl orthosilicate (0.2 g, 1.0 mmol) were dissolved of tetrahydrofuran (1.0 ml). Pure water and triethylamine as a catalyst were added dropwise to the solution. The mixture was then dried and cured at 40 °C for 3 h in a PTFE petri dish. Further cross-linking was carried out at 120 °C for 24 h. The cross-linked film was dipped in organic solvent to wash, and dried under vacuum. FT-IR (ATR, cm^{-1}): 3500 (–NH–), 2940 (–CH₂–), 1750 (–CO–O–).

Enzyme degradation of cross-linked films

To investigate the biodegradability of the cross-linked films, we performed enzymatic degradation of the obtained products using porcine pancreas lipase. The enzymatic degradation reaction was carried out for 30 days under suitable conditions (for example, phosphate buffer of pH 8.2) using porcine pancreas lipase. The specific methods are described below.

First, phosphate buffer was prepared by combining disodium hydrogen phosphate (8.95 g), potassium dihydrogen phosphate (0.91 g) and pure water (500 ml). Cross-linked films were cut into 1.0 cm² squares. The samples were weighed and dipped into the freshly prepared phosphate-buffered solution (30 ml) for 24 h in an Erlenmeyer flask equipped with a lid. The porcine pancreas lipase (1.0 g, 20 units) was then added to the flask and shaken for 30 days at 37 °C. At this point, the products were washed with pure water, dried under vacuum and weighed.

Measurements

Infrared absorption spectra (FT-IR) were measured using a JASCO FT/IR-615 instrument. ¹H NMR spectra were obtained using a MERCURY plus 400 MHz instrument by Varian Technologies Japan (Tokyo, Japan). NMR data are expressed in p.p.m. units relative to internal TMS. Molecular weights of the polymer were determined by gel permeation chromatography (GPC). Polystyrene was used as a calibration standard. GPC measurements were carried out with an HLC-8220 instrument (Tosoh, Tokyo, Japan) using a TSKgel Super HM-M column and DMF (*N,N*-dimethylformamide) as solvent/eluent. X-ray diffraction analysis was performed using a Rigaku (Tokyo, Japan) X-ray diffractometer. Stress-strain curves were measured at room temperature using an EZ-L 1.0 kN instrument by Shimadzu (Kyoto, Japan). Thermogravimetric analysis was conducted in air or nitrogen atmosphere using a Rigaku Thermoplus TG 8120 at a heating rate of 10.0 °C min⁻¹. The nitrogen flow was measured at 100 ml min⁻¹. DSC (differential scanning calorimetry) was performed using a Rigaku Thermoplus DSC 8230 at a heating rate of 10.0 °C min⁻¹. Dynamic mechanical analysis was performed on a DDV-GP instrument (A & D, Tokyo, Japan). Dynamic mechanical analysis measurements were carried out over four frequencies (1.0 Hz, 5.0 Hz, 10.0 Hz) at a heating rate of 2.0 °C min⁻¹.

RESULTS AND DISCUSSION

Synthesis of COLA (1)

The yield of COLA was 6.43 g (82%), and the product was soluble in common organic solvents, such as methanol, CHCl₃, and DMF; however, it was insoluble in hexane and water. The molecular weight and molecular weight distribution (M_w/M_n) of COLA were determined by GPC. The number-average molecular weight (M_n) and weight-average molecular weight (M_w) of COLA were determined to be 5320 and 6420 ($M_w/M_n = 1.20$), respectively. The structure of the product was confirmed by ¹H NMR spectroscopy. Peaks attributable to castor oil's alkyl group were found at 0.9 p.p.m. and 1.2–1.4 p.p.m. Furthermore, peaks attributable to the methyl and methine protons of PLLA, formed by the reaction of *L*-lactide with castor oil, were observed at 1.4–1.7 p.p.m. and 5.2 p.p.m., respectively. The castor oil methine peak at 3.5 p.p.m. disappeared, and a new peak at 4.9 p.p.m. appeared, confirming esterification of the castor oil. Accordingly, the products confirmed the structure of COLA. These results were identical with those observed in a previous study.¹⁹

Synthesis of products containing triethoxysilyl groups (2) and (3)
 CO-TES and COLA-TES were obtained in high yield (>95%). The products, both of which contain a triethoxysilyl group, exhibited similar solubility in organic solvents as COLA; both were also insoluble in hexane and water. The structures of both products were confirmed by ¹H NMR spectroscopy. The peaks for castor oil and COLA were confirmed. The peaks of the alkyl group of 3-(triethoxysilyl)propyl isocyanate were observed at 0.6 p.p.m. Moreover, peaks attributable to the methylene protons in the ethoxy group were confirmed at 3.8 p.p.m. The –NH– peaks derived from the urethane group were observed at 3.2 p.p.m. (Figure 2).

Preparation of cross-linked films

Cross-linked CO-TES (Film 1) was obtained as a colorless film in 61% yield. The film was easily broken when peeled off of the PTFE petri dish. Cross-linked COLA-TES (Film 2) was obtained as a white, self-supporting film in 57% yield. The cause of the coloration in Film 2 is presumably due to the crystalline moieties formed from the *L*-lactide segments. The film prepared using COLA-TES and tetraethyl orthosilicate (Film 3) was also white and self-supporting, which is in contrast to Film 1, and it was obtained in 71% yield. The coloration of Film 3 was similar to that of Film 2. The X-ray diffraction spectra of Film 2 and Film 3 both exhibited a characteristic peak at $2\theta = 16.5^\circ$, which was assigned to the presence of crystalline PLLA.⁶ The crystallinity of the films was calculated using the following equation (1):

$$\text{Crystallinity}(\%) = \frac{I_c}{I_c + I_a} \times 100 \quad (1)$$

where I_c represents the integrated intensity of the crystalline peaks and I_a represents the integrated intensity of the amorphous peaks. The crystallinity of Films 2 and 3 were calculated as 64 and 49%, respectively. Both films were found to be insoluble in organic solvents, likely due to the cross-linked nature of the products. FT-IR spectroscopy was used to estimate the molecular structure of the products. A signal at 3300 cm^{-1} –3500 cm^{-1} in all the three films confirmed the presence of –NH– moieties derived from the formation of urethane groups. Furthermore, a signal attributable to the amide NH was observed at 1530 cm^{-1} in the IR spectra of all the three films. The peak at 1100 cm^{-1} was attributed to the siloxane group, indicating the formation of polysilsesquioxane. The FT-IR spectrum of Film 2 is shown Figure 3.

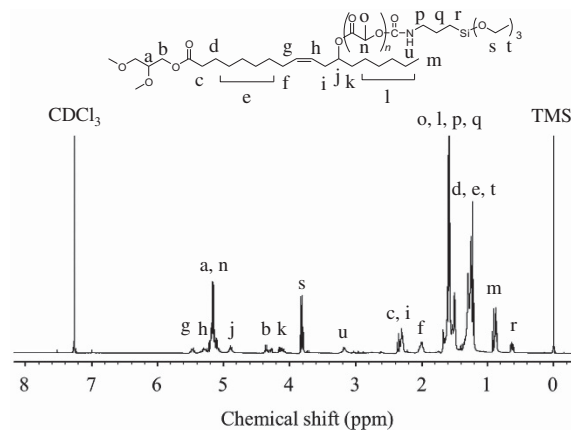


Figure 2 ¹H NMR spectrum of COLA-TES (3) in CDCl₃.

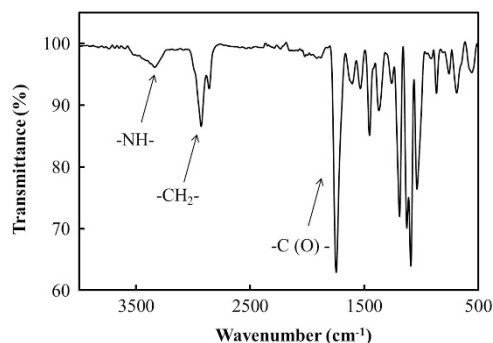


Figure 3 Fourier transform infrared spectrum of Film 2.

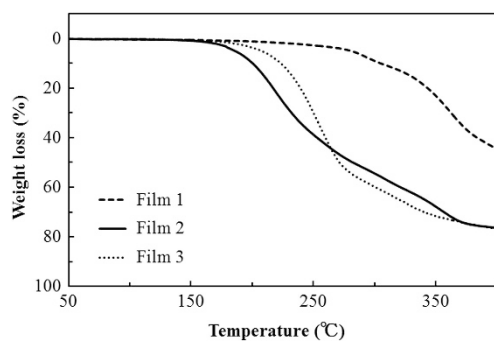


Figure 4 Thermogravimetric analysis curves of Film 1, Film 2 and Film 3 at a heating rate of 10 °C min^{-1} under a nitrogen atmosphere.

Thermal properties

To determine the thermal stability of the samples, thermogravimetric analysis was carried out under both nitrogen and air atmospheres. Figure 4 shows the thermogravimetric analysis curves for Films 1, 2 and 3 obtained under a nitrogen atmosphere. For Film 1, the temperature at which 5% weight loss occurred (T_{d5}) was 275 °C , and the temperature at which 10% weight loss occurred (T_{d10}) was 298 °C . For Film 2, the T_{d5} and T_{d10} were 186 and 200 °C , respectively. In addition, the melting temperature of the crystalline domain of Film 2 was observed at 133.2 °C in the DSC measurement. For Film 3, a T_{d5} of 208 °C and a T_{d10} of 223 °C was observed, and a melting temperature of the crystalline domain was observed at 127.9 °C in the DSC measurement. The thermal stabilities of the samples under an air atmosphere were similar to those measured under nitrogen protection (Table 1). In descending order, the thermal stabilities of the three films were found to be: Film 1 > Film 3 > Film 2. The thermal stability of the films is influenced by the L-lactide segment, which is sensitive to thermal degradation, as well as the inorganic content. For instance, Film 1 exhibited a higher thermal stability than Film 2 because Film 1 lacks L-lactide segments. The relatively low degradation temperature of Film 2 ($T_{d5} = 190\text{ °C}$) was presumably caused by network imperfections along the COLA side chain. Film 3 was more thermally stable than Film 2 because Film 3 has a higher inorganic content than Film 2.

Mechanical properties

We sought to further examine the mechanical properties of Films 2 and 3 upon observation that these samples peeled off easily from the PTFE petri dish. Presumably, Films 2 and 3 were able to be peeled from the PTFE petri dish because the interaction of the incorporated

Table 1 Thermal stability of cross-linked films

Compounds	Atmosphere	T_{d5}^a (°C)	T_{d10}^a (°C)
Film 1	Air	268	292
	N ₂	275	298
Film 2	Air	182	197
	N ₂	186	200
Film 3	Air	207	221
	N ₂	208	223

^aDetermined by thermogravimetric analysis measured at a heating rate 10 °C min^{-1} .

L-lactide segments increased their toughness. Thus, the mechanical properties of the films were further evaluated by stress–strain analysis. Figure 5 shows the stress–strain curves for Films 2 and 3. For Film 2, the tensile strength at break (T_B) was 1.92 MPa , and the elongation at break (E_B) was 61.2% . The Young's modulus (E) of Film 2 was 3.41 MPa . For Film 3, T_B , E_B and E were determined to be 0.28 MPa , 23.1% and 2.62 MPa , respectively. Overall, the mechanical strength of Film 3 was lower than Film 2. We hypothesized that the presence of the silsesquioxane moiety served to lower the crystallization of L-lactide segments, thereby leading to a decrease in mechanical strength.³⁴

We subsequently measured the dynamic viscoelastic properties of both films by dynamic mechanical analysis. Figure 6 shows the temperature dependence of storage modulus (E'), loss modulus (E'') and loss tangent ($\tan \delta$) of Film 2 at 1.0 Hz . The onset of the rubbery plateau region in E' of Film 2 was observed at 20 °C . This confirmed the stable elasticity of Film 2 at higher temperatures. Film 3 could not be measured at -100 °C and was therefore measured at -50 °C . The rubbery plateau region in the E' of Film 3 began at 15 °C ; however, Film 3 was broken at 90 °C . The reason for Film 3 breakage at both high and low temperature was considered to be caused by its low strength due to its silica content. The glass transition temperature (T_g) of Film 2 was observed at 3 °C , while the T_g of Film 3 was observed at -8 °C . The T_g s of both the samples were similar to that of a branched PLLA-based polymer film ($T_g = -5\text{ °C}$).¹⁹ These results suggest that both the samples are elastomers at room temperature.

Enzyme degradability

Weight loss (%), GPC and $^1\text{H NMR}$ spectra were measured for the films after a degradation period of 30 days. GPC measurements and $^1\text{H NMR}$ spectroscopy were carried out on the soluble portions of the samples. The weight loss (%) values, as well as the molecular weights of the degraded products as obtained by GPC, are shown in Table 2. The value of weight loss (%) was calculated using the following equation (2):

$$\text{Weightloss(\%)} = \frac{W_0 - W_{30}}{W_0} \times 100 \quad (2)$$

where W_0 represents the initial sample weight, and W_{30} represents the degraded sample weight.

The degradability of the films was thought to be caused by the L-lactide segments because Film 1, which does not contain any L-lactide, was not degraded. The degradability of Film 2 was similar to that of the branched PLLA-based polymer film (weight loss = 8.4%).¹⁹ We also carried out control experiments in the absence of lipase to evaluate the effect of lipase on film degradation. In the absence of lipase, Films 2 and 3 exhibited weight losses of 8.6 and 18.4% , respectively. These results suggested that the L-lactide segments

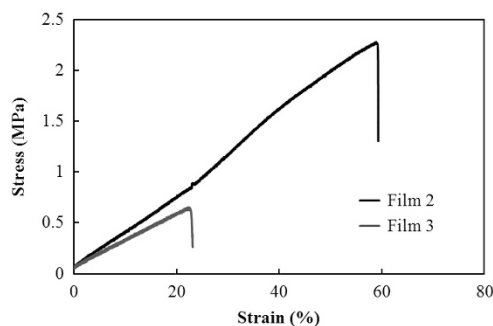


Figure 5 Stress-strain curves of Film 2 and Film 3.

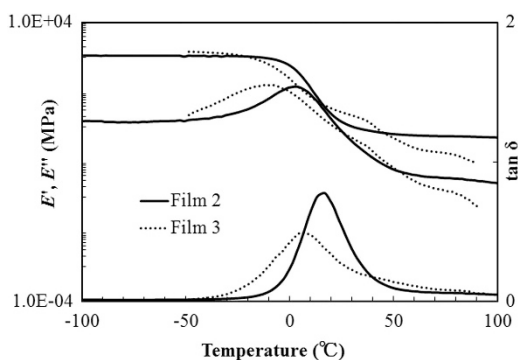


Figure 6 Temperature dependence of E' , E'' and $\tan \delta$ of Film 2 and Film 3.

were susceptible to degradation by phosphate buffer; however, the weight loss values were reduced in comparison with those obtained under the degradation conditions containing lipase. Because no degradation was observed for Film 1, the castor oil moiety in the polymer network was considered to be unaffected by the hydrolysis mechanisms promoted by the phosphate buffer and lipase. Because lipase is an enzyme that catalyzes the hydrolysis of triglycerides, we expected it to affect the castor oil moiety. In other words, we expected lipase to affect the triglycerides of the degradation products. Furthermore, Film 3 exhibited a higher degradability than Film 2, which was considered to be due to the lower crystallinity of the PLLA segments in Film 3 relative to Film 2.³⁵ GPC measurements of the degradation products of Films 2 and 3 revealed the presence of soluble polymers; the peaks observed in the GPC traces were attributed to free COLA (1). In contrast, no signals were found in the GPC trace of Film 1 after exposure to the degradation conditions, which further confirmed the results from the weight loss measurement that Film 1 was not degradable. Low molecular weight degradation products, such as lactic acid likely dissolved in the phosphate buffer. For both degraded Film 2 and degraded Film 3, the ¹H NMR spectra of the soluble portions revealed peaks attributable to COLA at 0.9–5.6 p.p.m. Furthermore, the peaks assignable to $-\text{CH}_2-\text{CH}_2-\text{Si}-$ at 0.6 p.p.m. were not observed. We therefore reasoned that the inorganic moiety remained inside the polymer network even after degradation. In addition, peaks attributable to the carboxylic acid protons derived from the degradation product were not observed in the expected range of 10–11 p.p.m. These results support the GPC measurements, which showed that degradation products dissolved in the phosphate buffer.

CONCLUSION

In conclusion, we prepared novel network polymers using castor oil and 3-(triethoxysilyl)propyl isocyanate. The obtained films were

Table 2 Weight loss and molecular weights of degraded products

Compounds	Weight loss (%)	M_n^a	M_w/M_n^a
Film 1	0	—	—
Film 2	9.2	3770	1.21
Film 3	21.3	4420	1.24

^aDetermined by gel permeation chromatography in *N,N*-dimethylformamide based on polystyrene standards.

insoluble in organic solvents due to its cross-linked structure. In descending order, the thermal stability (T_{d10}) of the three films was determined to be: Film 1 (298 °C) > Film 3 (223 °C) > Film 2 (200 °C). The interaction of the L-lactide segments increased the mechanical strength of the resultant film, while the presence of silsesquioxane moieties decreased the mechanical strength. Films 2 and 3 exhibited T_g s below room temperature. Collectively, these results confirm the high thermomechanical properties of Film 2. As such, we expect Film 2 to be useful in soft material applications, such as elastomers and synthetic leather. In addition, the degradability of the polymer films in the presence of lipase was confirmed. After 30 days of degradation time, the weights of both Film 2 and Film 3 decreased significantly, while Film 1 did not exhibit any weight loss.

CONFLICT OF INTEREST

The authors declare no conflict of interest.

ACKNOWLEDGEMENTS

We are grateful to Professor H. Honma, Kanto Gakuin University Materials and Surface Engineering Research Institute, Yokohama, Japan, for his helpful comments. We are grateful to Dr N. Takahashi, Kanto Gakuin University Yokohama, Japan, for determining the crystallinity of the samples. We thank Itoh Oil Chemicals for providing castor oil. This work was partly supported by a MEXT-Supported Program for the Strategic Research Foundation at Private Universities, 2012–2016.

- Nagata, M. & Sato, Y. Synthesis and properties of photocurable biodegradable multiblock copolymers based on poly(ϵ -caprolactone) and poly(L-lactide) segments. *J. Polym. Sci. A Polym. Chem.* **43**, 2426–2439 (2005).
- Petrović, Z. S., Guo, A. & Zhang, W. Structure and properties of polyurethanes based on halogenated and nonhalogenated soy-polyols. *J. Polym. Sci. A Polym. Chem.* **38**, 4062–4069 (2000).
- Yamaguchi, S., Tanha, M., Hult, A., Okuda, T., Ohara, H. & Kobayashi, S. Green polymer chemistry: lipase-catalyzed synthesis of bio-based reactive polyesters employing itaconic anhydride as a renewable monomer. *Polym. J.* **46**, 2–13 (2014).
- Hosoda, N., Tsujimoto, T. & Uyama, H. Biopolymers, bio-related polymer materials plant oil-based green composite using porous poly(3-hydroxybutyrate). *Polym. J.* **46**, 301–306 (2014).
- Murakami, S. & Aoki, N. Synthesis and ring-oligomer recovery of an environmentally benign malate-containing polyurethane using enzymatic process. *Kobunshi Ronbunshu* **70**, 565–571 (2013).
- Kaczmarek, H., Nowicki, M., Vuković-Kwiatkowska, I. & Nowakowska, S. Crosslinked blends of poly(lactic acid) and polyacrylates: AFM, DSC and XRD studies. *J. Polym. Res.* **20**, 91 (2013).
- Marubayashi, H., Asai, S., Hikima, T., Takata, M. & Iwaki, T. Biobased copolymers composed of L-lactic acid and side-chain-substituted lactic acids: synthesis, properties, and solid-state structure. *Macromol. Chem. Phys.* **214**, 2546–2561 (2013).
- Hadano, M., Yamaguchi, T., Otsuka, H., Aoi, K., Sasaki, S. & Takahara, A. Characterization and degradation behavior of segmented poly(urethaneurea)s prepared from lysine-based diisocyanate. *Nippon Gomu Kyokaishi* **79**, 219–224 (2006).
- Kojio, K. Research and development trend of biomass-based polyurethanes. *Nippon Gomu Kyokaishi* **86**, 176–180 (2013).
- Yokoe, M., Aoi, K. & Okada, M. Biodegradable polymers based on renewable resources. VII. Novel random and alternating copolycarbonates from 1,4:3,6-dianhydrohexitols and aliphatic diols. *J. Polym. Sci. A Polym. Chem.* **41**, 2312–2321 (2003).
- Mülhaupt, R. Green polymer chemistry and bio-based plastics: dreams and reality. *Macromol. Chem. Phys.* **214**, 159–174 (2013).
- Sharma, V. & Kundu, P. P. Condensation polymers from natural oils. *Prog. Polym. Sci.* **33**, 1199–1215 (2008).

- 13 Ristić, I. S., Marinović-Cincovic, M., Cakić, S. M., Tanasić, L. M. & Budinski-Simendić, J. K. Synthesis and properties of novel star-shaped polyesters based on l-lactide and castor oil. *Polym. Bull.* **70**, 1723–1738 (2013).
- 14 Tsujimoto, T., Haza, Y., Yin, Y. & Uyama, H. Synthesis of branched poly(lactic acid) bearing a castor oil core and its plasticization effect on poly(lactic acid). *Polym. J.* **43**, 425–430 (2011).
- 15 Miao, S., Zhang, S., Su, Z. & Wang, P. A novel vegetable oil-lactate hybrid monomer for synthesis of high-Tg polyurethanes. *J. Polym. Sci. A Polym. Chem.* **48**, 243–250 (2010).
- 16 Yachi, R. & Kouzai, H. Synthesis and properties of novel polyurethane from plant-based materials. *Mater. Sci. Tech. Jpn* **48**, 177–181 (2011).
- 17 Kamei, M., Kuratani, K. & Kouzai, H. Synthesis of novel polyurethanes by castor oil. *Mater. Raifu Gakkaishi* **20**, 156–159 (2008).
- 18 Uchida, N. & Kouzai, H. Synthesis of novel polyurethane with ricinoleic acid. *Mater. Sci. Tech. Jpn* **51**, 213–216 (2014).
- 19 Uchida, N. & Kouzai, H. Synthesis of novel UV-curable resin using castor oil with 2-acryloyloxyethyl isocyanate. *Kobunshi Ronbunshu* **72**, 76–81 (2015).
- 20 Minegishi, S., Tsuchida, S., Sasaki, M., Kameyama, A., Kudo, H. & Nishikubo, T. Synthesis of polyphosphonates containing pendant chloromethyl groups by the poly-addition of bis(oxetane)s with phosphonic dichlorides. *J. Polym. Sci. A Polym. Chem.* **40**, 3835–3846 (2002).
- 21 Nakabayashi, N. & Kanda, K. Synthesis of phosphoric compounds and their adhesives to bovine teeth. *Kobunshi Ronbunshu* **45**, 91–96 (1988).
- 22 Sakagami, Y., Horiguchi, K., Narita, Y., Sirithep, W., Morita, K. & Nagase, Y. Syntheses of a novel diol monomer and polyurethane elastomers containing phospholipid moieties. *Polym. J.* **45**, 1159–1166 (2013).
- 23 Maehara, T., Ohshita, J., Taketsugu, R., Hino, K. & Kunai, A. Hydrosilylation polymerization for the synthesis of organosilicon polymers containing adamantane units. *Polym. J.* **41**, 973–977 (2009).
- 24 Kuratani, K., Hasegawa, S., Katsumata, T. & Kouzai, H. Synthesis of phosphate esters containing polymers having mesogenic group in the side chains. *Kobunshi Ronbunshu* **65**, 188–191 (2008).
- 25 Tanaka, K. & Chujo, Y. Material development of the network polymer and silicon-based hybrid polymer. *J. Netw. Polym. Jpn* **32**, 233–244 (2011).
- 26 Nagafuchi, K., Kashio, M., Sugizaki, T. & Moriya, O. Synthesis of amphiphilic and thermoresponsive polysilsesquioxane through ring opening reaction of succinimide group. *Kobunshi Ronbunshu* **72**, 48–56 (2015).
- 27 Takamura, N., Okonogi, H., Gunji, T. & Abe, Y. Preparation and properties of polysilsesquioxanes preparation and properties of polymer hybrids from vinyltrimethoxysilane. *Kobunshi Ronbunshu* **54**, 198–207 (2000).
- 28 Karadag, K., Onaran, G. & Sonmez, H. B. Polymer synthesis and reactions synthesis of crosslinked poly(orthosilicate)s based on cyclohexanediol derivatives and their swelling properties. *Polym. J.* **42**, 706–710 (2010).
- 29 Niida, K., Yamaguchi, M., Kashio, M., Sugizaki, T., Moriya, O. & Kageyama, T. Polysilsesquioxane having glycidyl group as a new hybrid adhesive material. *J. Adhes. Soc. Jpn* **46**, 203–208 (2010).
- 30 Kim, K., Ogoshi, T. & Chujo, Y. Controlled polymer hybrids with ladderlike polyphenylsilsesquioxane as a template via the sol-gel reaction of phenyltrimethoxysilane. *J. Polym. Sci. A Polym. Chem.* **43**, 473–478 (2005).
- 31 Sugizaki, T., Kashio, M., Kimura, A., Yamamoto, S. & Moriya, O. Graft polymerization of polysilsesquioxane containing chloromethylphenyl groups by atom transfer radical polymerization. *J. Polym. Sci. A Polym. Chem.* **42**, 4212–4221 (2004).
- 32 Lin, Y., Pramoda, K. P., He, C., Chen, W. & Chung, T. S. Synthesis of poly(phenylsilsesquioxane) having organostannyl groups. *J. Polym. Sci. A Polym. Chem.* **39**, 2215–2133 (2001).
- 33 Tsujimoto, T., Uyama, H. & Kobayashi, S. Green nanocomposites from renewable resources: biodegradable plant oil-silica hybrid coatings. *Macromol. Rapid Commun.* **24**, 711–714 (2003).
- 34 Nanbu, S. & Kuraoka, K. Preparation and characterization of silica/poly (butylenesuccinate-co-adipate) organic-inorganic hybrid biodegradable materials by sol-gel method. *J. Pac. Sci. Technol.* **18**, 331–340 (2009).
- 35 Inoue, Y. *Research and Development for Green Plastics* 154 (CMC Publishing, Japan, 2002).